International Series of Numerical Mathematics, Vol. 149, 195–208

Continuum Models for Surface Growth

Martin Rost

Abstract. As an introductory lecture to the workshop an overview is given over continuum models for homoepitaxial surface growth using partial differential equations (PDEs). Their *heuristic derivation* makes use of inherent symmetries in the physical process (mass conservation, crystal symmetry, ...) which determines their *structure*. Two examples of applications are given, one for large scale properties, one including crystal lattice discreteness. These are: (i) a simplified model for *mound coarsening* and (ii) for the transition from *layer-by-layer* to *rough growth*. Virtues and shortcomings of this approach is discussed in a concluding section.

Mathematics Subject Classification (2000). Primary 82B26; Secondary 35K35.

Keywords. Surface evolution; mound coarsening; roughening transition.

1. Introduction

Crystal growth by Molecular Beam Epitaxy (MBE) involves processes on quite different physical scales, from atomic to micrometer scales. To capture the large scale features it may be appropriate to represent the surface as a continuous height field $h(\mathbf{x}, t)$ above a set of so called base points $\mathbf{x}$ where $h : (\mathbf{x}, t) \in \mathbb{R}^2 \times \mathbb{R} \to \mathbb{R}$. The surface dynamics is then modeled by a parabolic PDE for $h(\mathbf{x}, t)$, which often is a starting point for interesting mathematical problems, and in some cases for rigorous results [1, 2], which were an important part of this workshop.

Their mathematical tractability somehow contrasts with the lack of rigor in their derivations, as we shall see below. It would be nice to "prove" a certain PDE to be the appropriate large scale model for some underlying more elementary model, typically a stochastic model of the solid-on-solid type. This would connect the result for large scales with the microscopic model which is much closer to physical reality.

Nevertheless, often this chain can be closed in a heuristic sense, and this lecture presents some examples. It is organised as follows: First, the heuristic procedure of deriving a continuum model is motivated and its structure is explained.

Then, two examples of applications are presented, covering in some sense extreme cases of applicability of continuum models; (i) coarsening of mound patterns in homoepitaxy and (ii) damping of width oscillations in the transition from layer-by-layer to rough growth. Last, the general applicability of continuum models to MBE growth is discussed, in particular those features of discreteness of the underlying process which can only be covered incompletely by a continuum model. Open questions in the derivation which have not been addressed so far, but appear to be solvable, are mentioned here.

The main purpose of this introductory lecture is to recollect the physical motivation of the class of models which deal with the largest spatial and temporal scales involved in MBE growth, and to give some intuition to other more mathematical approaches.

2. Derivation and structure

2.1. General background

Continuum models for surface growth are comparable to the hydrodynamic limit of microscopic models of fluid dynamics. Behind the continuous macroscopic height field $h(\mathbf{x}, t)$ one has to imagine an ensemble of microscopic configurations. They may be locally in a steady state or, in growth modes where the crystal layer structure is relevant such as layer-by-layer or step flow growth, a sequence of states may repeat itself periodically. On time scales larger than the layer completion time also the latter case may be considered a quasi-steady state. Figure 1 illustrates this relationship. The local state is subject to changes on time scales, ideally longer than the relaxation times into those states, which leads to the dynamics of the height field.

The structure of the PDE governing the dynamics of $h(\mathbf{x}, t)$ reflects different elementary processes and their symmetries. In growth from molecular beam epitaxy there is

- a deposition flux $F_{\{h\}}(\mathbf{x}, t)$, i.e., the deposited volume per time and surface area,
- possibly an evaporation loss $E_{\{h\}}(\mathbf{x}, t)$, again volume per time and area,
- a surface current $\mathbf{J}_{\{h\}}(\mathbf{x}, t)$ on terraces and along steps, transported volume per time and length, i.e., cross section on the surface.

Multiplied with a volume density ρ these quantities become mass fluxes and currents. All three depend on the actual surface configuration h, e.g., on local slopes, their orientations and curvatures. Elastic interactions and terrace adatom detachment with subsequent redeposition couple the dynamics at a surface point *non-locally* to surface configurations at other places. There may also be an *explicit* space dependence beyond the influence of the height configuration, e.g., for a non-uniform deposition with pulsed flux.

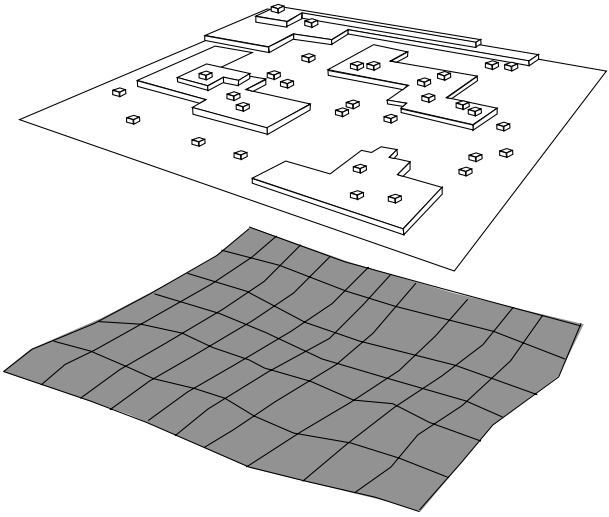

FIGURE 1. Sketch of the height field representation for surface configurations. Upper: one surface configuration out of an ensemble in local steady states. Lower: a smooth height field $h(\mathbf{x}, t)$ as a representation.

Deposition, evaporation, and surface current are combined into a *continuity equation*

$$\frac{\partial}{\partial t}\, h(\mathbf{x}, t) = F_{\{h\}}(\mathbf{x}, t) - \nabla \cdot \mathbf{J}_{\{h\}}(\mathbf{x}, t) - E_{\{h\}}(\mathbf{x}, t). \tag{2.1}$$

Note that small local slopes are assumed, such that in front of the surface current divergence nonlinear terms arising from the metric $\sqrt{1+(\nabla h)^2}$ typically are neglected.

A full derivation from local steady states in the sense postulated above is of course impossible in almost any case, apart from some one-dimensional examples related to growth models, as, e.g., [3], which is however not of MBE type. One therefore has to rely on heuristically justified (*reasonable*) assumptions for the dynamic quantities involved. The connection to the more detailed models on smaller scales is given by length scales which influence the surface morphology and become visible. Explained more precisely in the other introductory lectures of this conference [4, 5] they are

- a, the lattice spacing of the crystal.
- ℓ_{D}, the diffusion length, i.e., the "typical" distance of nucleation sites on a terrace, with a non-trivial dependence on the deposition rate F and adatom diffusivity D.
- $\ell_{\mathrm{ES}} = a\big[\exp \varepsilon_{\mathrm{ES}} - 1\big]$, the Ehrlich–Schwoebel length [6]. $\varepsilon_{\mathrm{ES}}$ is the magnitude of the Ehrlich–Schwoebel barrier in units of $k_{\mathrm{B}}T$. It is a measure for the reflectivity of the barrier at a downward step. Roughly speaking, an adatom

located right at a downward step is equally likely to hop downward as it is to get caught by the next upward step at distance $\ell_{\rm ES}$.
- $\ell_{\rm step}$, the average distance between two truly ascending step without counting islands etc. between them. So, a slope $|\mathbf{m}|$ of a vicinal surface is equivalent to $\ell_{\rm step} = a/|\mathbf{m}|$.

2.2. Surface current

Ehrlich–Schwoebel effect on terraces

As was realised quite early the most important ingredient of Eq. (2.1) is a non-equilibrium current on surface terraces induced by Ehrlich–Schwoebel (ES) barriers [7, 8, 9, 11].

For small average slopes $\mathbf{m} = \nabla h$ with $|\mathbf{m}| \ll a/\ell_{\rm D}$ or $\ell_{\rm D} \ll \ell_{\rm step}$, the ES barrier induces a net uphill current [25]

$$\mathbf{J}_{\rm EST} = \frac{F\ \ell_{\rm D}\ell_{\rm ES}}{2a(1+\ell_{\rm ES}/\ell_{\rm D})}\ \mathbf{m}. \tag{2.2}$$

Inserted into the surface current in Eq. (2.1) this results in a *destabilising* term for the height equation $\partial_t h = -c\,\nabla\cdot\nabla h + \cdots$.

Of course one would like to know the functional dependence of the surface current $\mathbf{J}_{\rm EST}$ beyond this approximation for small slopes. Following an argument of Siegert for $1+1$ dimensions [9] there must also be surface orientations with stabilising surface current: Think of $\mathbf{J}_{\rm EST}$ as a vector field on the tangent bundle of the unit sphere of possible surface orientations. By the ES instability all high symmetry orientations have $\mathbf{J}_{\rm EST}$ pointing outward around a zero. By continuity of $\mathbf{J}_{\rm EST}$ as a function of the orientation there must be zeroes with the current field pointing inward to the zero, i.e., orientations stabilised by the surface current.

These qualitatively fundamental properties, the existence of unstable and stable surface orientations, can be cast into a heuristically postulated function $\mathbf{J}_{\rm EST}(\mathbf{m})$. Figure 2 shows two such examples, one isotropic within the crystal terrace – a somewhat artificial but nevertheless theoretically interesting case, one isotropic, with four-fold ($\pi/2$) rotational symmetry.

Ehrlich–Schwoebel effect at steps

The Ehrlich–Schwoebel effect also has an influence on adatom diffusion along steps, allowing for attachment of atoms to kinks preferentially from one side, as is sketched in Fig. 3. It is one important mechanism causing a step meandering instability on growing vicinal surfaces [12, 13]. Politi and Krug derived the contribution $\mathbf{J}_{\rm ESS}$ of non-equilibrium current along steps to the total surface current for a surface with given average slope which is assumed to be constant on a sufficiently large region such that steps have a well defined average density and orientation with respect to the underlying crystal lattice [14].

Curvature relaxation

Clearly on small scales the destabilising ES effects encountered in this section so far are balanced. Too thin protrusions are forbidden by their cost in surface free

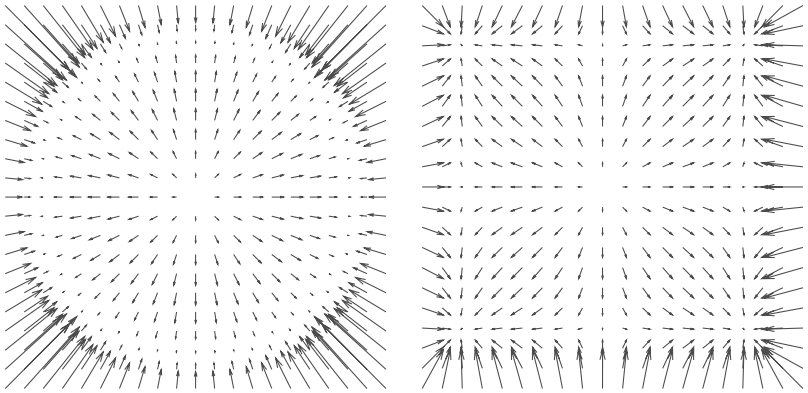

FIGURE 2. Examples of heuristic choices for nonequilibrium terrace Ehrlich–Schwoebel surface current $\mathbf{J}_{\mathrm{EST}}(\mathbf{m})$. Left: in-plane isotropy, $\mathbf{J}_{\mathrm{EST}}(\mathbf{m}) = (1 - |\mathbf{m}|^2)\ \mathbf{m}$, continuous set of stable slopes $\{\mathbf{m} \mid |\mathbf{m}| = 1\}$. Right: anisotropy, four-fold symmetry, $J_{\mathrm{EST},i}(\mathbf{m}) = (1 - m_i^2)\ m_i$ with $i = x, y$, discrete set of stable slopes at $(\pm 1, \pm 1)$.

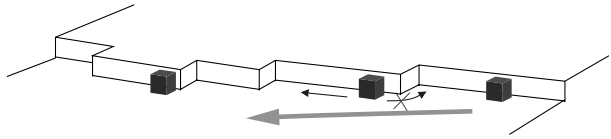

FIGURE 3. The ES effect at step kinks favors adatom incorporation from one side and induces a net current along the step.

energy. For thermal relaxation towards equilibrium the corresponding continuum dynamics are straightforward to derive. The surface free energy

$$\mathcal{F} = \int \gamma(\nabla h)\ \sqrt{1 + (\nabla h)^2}\ d^d x \tag{2.3}$$

weights each surface element by its orientation dependent contribution $\gamma(\nabla h)$. The gradient in chemical potential $\mu = \delta\mathcal{F}/\delta h$ drives the relaxational surface current which is also proportional to the (tensorial and orientation dependent) adatom mobility $\boldsymbol{\sigma}(\nabla h)$. A linear expansion around a surface of constant slope $h = \mathbf{m} \cdot \mathbf{x}$ small enough to again neglect geometric effects [10, 11] yields

$$\mathbf{J}_{\mathrm{CURV}} = \boldsymbol{\sigma} \cdot \nabla\ \nabla \cdot [\gamma\ \mathbf{1} + (\nabla_{\mathbf{m}} \nabla_{\mathbf{m}} \gamma)] \cdot \nabla h. \tag{2.4}$$

The expression in square brackets is generally called the surface *stiffness*

$$\tilde{\boldsymbol{\gamma}} = \gamma\ \mathbf{1} + \nabla_{\mathbf{m}} \nabla_{\mathbf{m}} \gamma \tag{2.5}$$

where $\nabla_{\mathbf{m}}$ denotes derivation with respect to the slope dependence of γ and $\mathbf{1}$ is the unity matrix.

Strictly speaking this derivation applies only to *equilibrium relaxation*. For a far from equilibrium process like MBE growth it does not make sense to define a surface free energy per area $\gamma(\nabla h)$, although the "true" contribution of the surface current due to relaxation by curvature most likely has a functional form of that type. Some attempts to identify these contributions have been made [15], but the correct derivation of the corresponding continuum form remains an open question.

2.3. Deposition, desorption and noise

For most applications it will be correct to assume a *deposition* intensity F constant in time and space. Interesting cases with *explicit* space and time dependence are (i) pulsed molecular beams, used to decrease the second layer island nucleation rate, and (ii) geometric inhomogeneities if the beam does not reach every part of the surface under the same angle. The most important mechanism for *implicit* deposition heterogeneity is steering, where the incident atoms are deflected by attractive interaction with surface features such as islands and mounds, an effect which is of course most prominent under grazing incidence [16, 17].

At sufficiently high temperatures *desorption* may become an important effect. Terrace adatoms then will be most susceptible to desorption at a rate $1/\tau$, during their diffusion time before they reach the stronger binding steps. To a first approximation the desorption rate depends on the average distance to the next reachable step and therefore on the surface slope: the higher the slope, the more steps are present and the lower the desorption loss. Within an ansatz à la Burton–Cabrera–Frank [18] one can relate the desorption length $x_\mathrm{s} = 2a\sqrt{D\tau}$, diffusion length ℓ_D, and slope $\nabla h = a/\ell$ [19, 11] to an expression for the desorption loss in volume per time and surface area

$$E_{\{h\}}(\mathbf{x},t) = F\ [(x_\mathrm{s}/\ell)\tanh(\ell/x_\mathrm{s}) - 1] \approx F\ \frac{(\ell_\mathrm{D}/x_\mathrm{s})^2/3}{1+(\nabla h)^2}. \tag{2.6}$$

There are three sources for *noise* in MBE growth [21]: (i) Deposition is a stochastic process of single events, so F has to be complemented by a "shot noise" term $\xi(\mathbf{x},t)$ with statistics

$$\langle \xi(\mathbf{x},t)\rangle = 0 \quad \text{and} \quad \langle \xi(\mathbf{x},t)\xi(\mathbf{x}',t')\rangle = a^3 F\ \delta(\mathbf{x}-\mathbf{x}')\ \delta(t-t'). \tag{2.7}$$

(ii) Adatom diffusion also consists of single events, and to a first approximation surface currents are blurred by a "diffusion noise" term $\boldsymbol{\eta}(\mathbf{x},t)$ with statistics

$$\langle \boldsymbol{\eta}(\mathbf{x},t)\rangle = 0 \quad \text{and} \quad \langle \boldsymbol{\eta}(\mathbf{x},t)\cdot\boldsymbol{\eta}(\mathbf{x}',t')\rangle = \ell_\mathrm{D} F\ \nabla^2\delta(\mathbf{x}-\mathbf{x}')\ \delta(t-t'). \tag{2.8}$$

(iii) Nucleations also occur at random but the precise form of this contribution remains an open question. There are nontrivial correlations in time, as new islands tend to nucleate close to centers of previously nucleated islands. The space dependence of the nucleation noise correlator $\langle \nu(\mathbf{x},t)\nu(\mathbf{x}',t')\rangle$ is expected to have the form $(\nabla^2)^2\delta(\mathbf{x}-\mathbf{x}')$ [22].

2.4. Structure and symmetry of continuum equations for MBE

Heuristic surface currents as in the example in Fig. 2 lead to a symmetry in the resulting dynamical equation which can be used for evaluation, but is too strong a restriction compared to the "real" dynamics and may lead to erroneous results.

If $\mathbf{J}_{\mathrm{EST}}$ uniquely depends on the slope $\mathbf{m}$ and not on derivative of its functions then a fourfold or sixfold crystal symmetry in the terrace layers imposes $\mathbf{J}_{\mathrm{EST}}(\mathbf{m}) = -\mathbf{J}_{\mathrm{EST}}(-\mathbf{m})$. (A threefold symmetry plays a special role [23]). The resulting term of surface dynamics is invariant under the transformation $h \to -h$ and so will be the surface configurations obtained from that. Breaking of this symmetry, e.g., by terms as $\nabla f\left((\nabla h)^2\right)$ in $\mathbf{J}$ or an evaporation term $e(\left((\nabla h)^2\right)$ do in fact change the characteristics of the dynamics substantially [19].

One can take advantage of this simple slope dependence if there is a scalar function $V(\mathbf{m})$ such that $\mathbf{J}_{\mathrm{EST}} = -\nabla_{\mathbf{m}} V(\mathbf{m})$. Stable zeroes of $\mathbf{J}_{\mathrm{EST}}$ then are minima of $V(\mathbf{m})$. If additionally the curvature relaxation is of a simple "scalar" form $\boldsymbol{\sigma} \cdot \tilde{\boldsymbol{\gamma}} = K\mathbf{1}$ there is a Lyapunov functional of the dynamics

$$\mathcal{F}\{\mathbf{m}\} = \int \left[\frac{K}{2}(\nabla \mathbf{m})^2 + V(\mathbf{m})\right] d^2x \tag{2.9}$$

and the surface dynamics Eq. (2.1) can be written for the field of slopes $\mathbf{m} = \nabla h$ as

$$\partial_t \mathbf{m} = \partial_t(\nabla h) = \nabla\, \nabla \cdot \frac{\delta \mathcal{F}}{\delta \mathbf{m}}. \tag{2.10}$$

If $\mathbf{m}$ is interpreted as a two-dimensional magnetic order parameter this form compares to conserved (model B) relaxational dynamics, with the only restriction that it remains a conservative field at all times, $\nabla \wedge \mathbf{m} = 0$. Facets in the surface are regions of constant slope, and appear as domains of constant "magnetisation", edges between them are domain walls. As compared to its magnetic analogon, here the parallel component of $\mathbf{m}$ remains constant across a domain wall, which in the case of discrete stable zeroes of the current function (right panel of Fig. 2) restricts the possible domain wall orientations and imposing constraints on the relaxational dynamics [24, 9, 23].

3. Examples of applications

Continuum equations are now applied in two examples of very basic choices in Eq. (2.1). In some sense they highlight two opposite regimes, (i) on very long length and time scales coarsening of mounds in homoepitaxy, and (ii) on short scales resolving the lattice structure in the transition from layer-by-layer to rough growth.

3.1. Coarsening

The simplest example of a surface dynamics equation is the analogon to the classical XY-model in the sense of Eq. (2.10)

$$\partial_t h = -(\nabla^2)^2 h - \nabla \cdot \left[\left(1 - (\nabla h)^2\right)\, \nabla h\right], \tag{3.1}$$

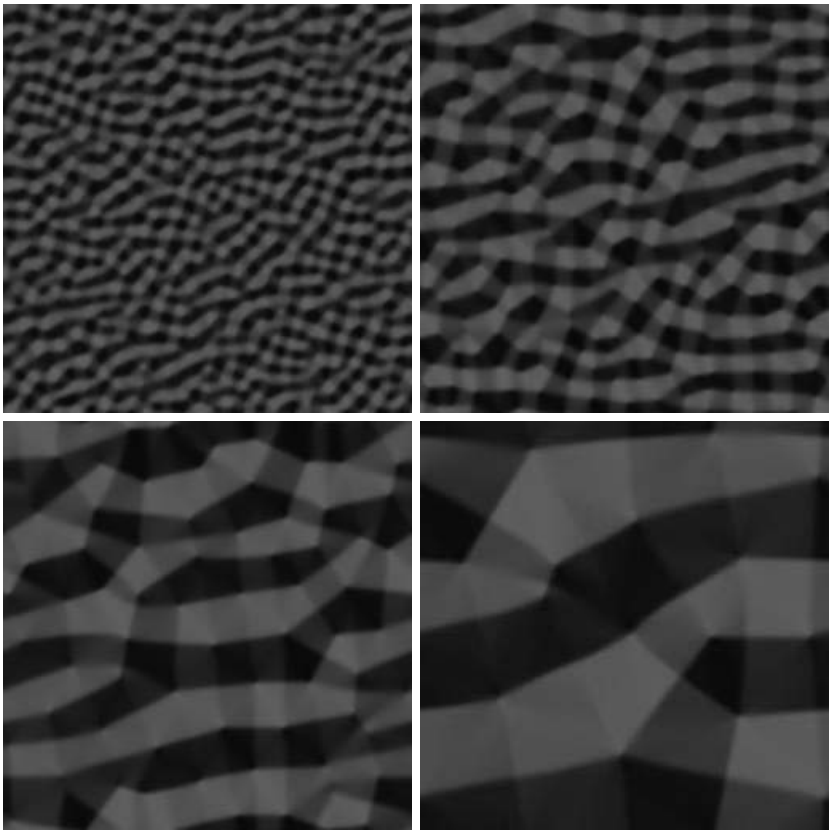

FIGURE 4. Coarsening of surface mounds, between subsequent panels time advances by a factor of 10. The local surface slope is represented by colors, facets appear as regions of uniform color. Spontaneous facet formation, although no anisotropy is imposed, $\mathbf{J}_{\mathrm{EST}}(\mathbf{m}) = (1 - |\mathbf{m}|^2)\,\mathbf{m}$ (c.f. left panel in Fig. 2).

i.e., with the current function depicted in the left panel of Fig. 2. An initially flat surface $h = const$ is linearly unstable to fluctuations of wave lengths $\lambda > 2\pi$ which therefore initially grow exponentially. Once slopes of $O(1)$ are reached the surface organise itself into a pattern of regular mounds and troughs which keep the symmetry $h \leftrightarrow -h$ of Eq. (3.1). The in-plane isotropy of (3.1) is locally broken by the need to arrange the mounds and troughs into a regular pattern and facets with sharp wedges form [25].

Subsequently the pattern of mounds and troughs coarsens keeping a single typical length scale and a statistically self similar pattern at every time. The average mound size is found to increase with time as $L \sim t^{1/3}$ [24, 23]. In a weak

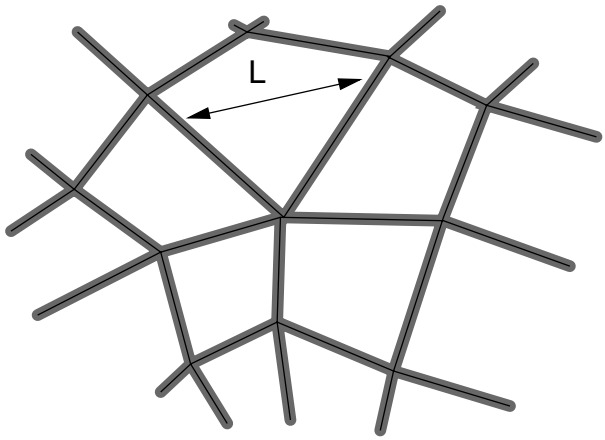

FIGURE 5. Sketch of facets and wedges, i.e., domains of constant slope and their separating boundaries, as obtained in the simulations shown in Fig. 4. The only macroscopic length scale is the domain size L.

sense this can be proved as an upper bound for an appropriate time average of the length scales L observed up to a give time t [2]. Here only a quick handwaving argument is given following [26]:

The spatial average of the interface width $W \equiv \langle h^2 \rangle$ (where $\langle h \rangle = 0$) increases due to Eq. (3.1) as

$$\frac{1}{2}\,\partial_t W^2 = \frac{1}{2}\,\partial_t \langle h^2 \rangle = -\langle (\Delta h)^2 \rangle + \langle (\nabla h)^2 \rangle - \langle |\nabla h|^4 \rangle. \tag{3.2}$$

By the sketch of Fig. 5 the contributions of these terms are estimated to be of order $1/L$: The facets are flat and the curvature is restricted to narrow strips of width $O(1)$ at the domain boundaries, which have a relative weight of $1/L$. Also, here the slopes are smaller than the stable value $|\nabla h| = 1$ attained at the facets. So all terms give a contribution of $O(1/L)$ and because of the stable slope $W \sim L$ the increase in width leads to the estimate

$$\partial_t L^2 \sim \partial_t W^2 \sim 1/L, \quad \text{integrated to} \quad L \sim t^{1/3}. \tag{3.3}$$

The same rough heuristic argument holds for anisotropic surface currents with discrete minima, i.e., a discrete set of preferential surface orientations, but the four-fold symmetry (right panel of Fig. 2) plays a special role because two kinds of edges occur, such that in general the assumption of a single length scale L in the system is wrong [23].

Clearly, Equation (3.1) is far from experimental realisations, and it is interesting by its challenge for mathematical, analytic and numerical methods.

Numerically, the coarsening exponent is found correctly only if one goes to very late times, when asymptotic mound sizes of at least 10 times the initial most

unstable wave length are reached [24]. Following [23], it may be interesting to verify the absence of any macroscopic length scales other than the mound size, e.g., to check possible orientational long range ordering of the mounds. This may require quite involved methods to avoid any artificial anisotropy from numerical lattices.

Mathematically, an improvement on the analysis of [2] is desirable but probably difficult to obtain. Physical intuition would call for a bound on the length scale $L(t)$ itself rather than its "history average" $\int_0^t L(s)ds$. It may be possible to obtain dynamical equations for the movements and merging of the singular points in the pattern of Fig. 4), for its maxima, minima, and saddle points. Such analysis has proven very helpful in 1+1 dimensions, e.g., [1, 27], and for anisotropic (2+1)-dimensional models, e.g., [23].

As the dynamics of these singular features play a crucial role, it is important to study their change in the presence of additional terms in Eq. (3.1). Based on analytic arguments assisted by simulations, noise is known to cause coarsening or to determine its properties [28]. Other additional nonlinear terms influence the morphology of the mound pattern, such as slope dependent evaporation [19], or other terms breaking up-down symmetry as $\nabla^2(\nabla h)^2$ [20]. A more difficult task may be the study of nonlinearities in prefactors to the smoothing term $-\Delta^2 h$ of Eq. (3.1).

3.2. Roughening

Layer by layer growth is technologically interesting because one can monitor the subsequent deposition of layers by oscillations in the surface width. It is nearly flat around integer fillings and the roughness takes maxima at half integer fillings. During growth the interface roughens and the width oscillations decay [29]. The Ehrlich–Schwoebel barrier and mounding instability is one prominent mechanism destroying layer-by-layer growth, and so can be any inhomogeneity in the deposition intensity $F_{\{h\}}(\mathbf{x}, t)$. Although weaker, even the fluctuations of shot noise have this effect, and it can be captured by a simple renormalisation group calculation.

The simplest way to implement layer lattice effects into an continuum surface equation like Eq. (2.1) is pursued by the conserved *sine-Gordon*-equation

$$\partial_t h(\mathbf{x}, t) = -K\Delta^2 h(\mathbf{x}, t) - V\Delta \sin \frac{2\pi h(\mathbf{x}, t)}{a_\perp} + F + \xi(\mathbf{x}, t). \tag{3.4}$$

Among other the surface current is driven to regions of incomplete fillings such that $h(\mathbf{x}, t)/a_\perp$ is favored to take integer values [30]. The notation distinguishes between the lattice constant normal ($a_\perp$) and parallel ($a_\parallel$) to the surface terraces which will be used in the following analysis.

In a momentum shell renormalisation one can average over the fluctuations caused by the short wavelength components of the noise, $\xi = \bar{\xi} + \delta\xi$, where $\bar{\xi}$ only contains modes of wavenumber smaller than some cutoff Λ and $\delta\xi$ the others. One now tries to approximate the dynamic equation for the averaged height field $\bar{h} = \langle h \rangle_{\delta\xi}$ by an equation like (3.4) with suitably adjusted parameters. After

rescaling, an effective *renormalised* equation is obtained. Three important physical interpretations can be obtained from the renormalised parameters of Eq. (3.4).

(i) by the interplay of the driving force F and the lattice potential the up-down symmetry ($h \leftrightarrow -h$) is broken and a term $-\lambda\Delta(\nabla h)^2$ is created.

(ii) The strength of the lattice potential V is damped out and decays exponentially with coverage $\theta = Ft$ like $\propto \exp\left(-a_\parallel^2/\ell_\mathrm{D}^2\sqrt{\theta}\right)$

(iii) In a sample of finite size Λ momentum shell renormalisation stops at minimal wavenumbers $|\mathbf{k}| = 2\pi/\Lambda$ and corresponding coverages $\theta = (\Lambda/\ell_\mathrm{D})^4$. The lattice potential therefore remains present in the renormalised large scale description if $\Lambda \ll \tilde{\ell} = \ell_\mathrm{D}^2/a_\parallel$, where $\tilde{\ell}$ is called *layer coherence* length [29, 30]. Expressed in more physical terms: shot noise fluctuations cannot accumulate to the point where width oscillations are completely blurred.

4. Discussion

In presenting the model derivations and examples of their application it becomes clear that continuum models are a good tool for questions where the inherent *simplifications* are justified. The insight gained from partial differential equations is different from results of more microscopic model. Last not least continuum equations can handle larger systems and longer times than Monte Carlo simulations or Molecular Dynamics.

In many cases the phenomena of particular technological interest cannot be captured by continuum equations of the type described in this lecture. Magic island shapes, surface reconstruction, certain aspects of step bunching, formation of quantum dots and wires are just a few examples.

Even if one is not interested in these inherently discrete phenomena themselves they nevertheless carry over to the behavior on larger scales and a naive straightforward derivation of large scale continuum models may be wrong. The implementation of noise for some questions, such as roughening, is one such example. Also, the effective "large scale" Ehrlich–Schwoebel barrier of a step is influenced by kinks along the step which may serve as channels for downward incorporation of a terrace adatom. Obtaining the correct effective barrier, dependent on orientation and curvature of the step certainly is a nontrivial task.

An important part of the surface current $\mathbf{J}$ flows along steps, as has become clear in the above derivation. In Ref. [14] the step current due to kink ES barriers is derived as a function of the surface orientation or slope. An open question is the role of step curvature and therefore of surface curvature on the step current.

Also on the surface itself, the regularising term as it is derived in Eq. (2.4), should be derived from true nonequilibrium arguments. To do so, one would have to incorporate island nucleations, the creation and annihilation of steps. One possible approach is to introduce fields for the densities of adatoms, advacancies, steps, kinks, and for their orientations. Locally they could be treated as mean

field densities with certain effective "reaction" rates, but in their spatial interaction, by diffusion and advective transport, one could obtain a conceptually more fundamental continuum model for surface growth.

5. Conclusion

In this lecture an overview of continuum models for MBE surface growth has been given which includes

- the conceptual foundation of continuum models as a limit of more detailed small scale approaches,
- heuristic derivations due to lack of rigorous or even exact ways to obtain them,
- the structure and the symmetry of the equations obtained in that way,
- two examples emphasizing two opposite time limits in the growth process with the application of two contrary methods,
- criticism of weak points in continuum modelling, open questions and some speculations about answers to them.

The main purpose was to highlight the physical background and give some intuition of possible approaches to it as a basis for mathematical treatments, both rigorous and numerical. It should be seen as a complement of the lectures [4] and [5] which give a similar introduction to lattice and Burton–Cabrera–Frank models respectively. Although continuum models seem to fail in some important physical aspects they nevertheless are a good tool and subject for mathematical approaches.

Acknowledgement

This work, as well as the participation at the workshop was supported by the Deutsche Forschungsgemeinschaft through the SFB "Singular Phenomena and Scaling in Mathematical Models" at the University of Bonn.

References

[1] R.V. Kohn and F. Otto, *Upper bounds on coarsening rates*, Comm. Math. Phys. **229** (2002) 375–395.

[2] R.V. Kohn, X.D. Yan, *Upper bound on the coarsening rate for an epitaxial growth model*, Comm. Pure Appl. Math. **56** (2003) 1549–1564.

[3] B. Derrida, E. Domany, and D. Mukamel, *An exact solution of the one dimensional asymmetric exclusion model with open boundaries*, J. Stat. Phys. **69** (1992) 667–687; G. Schütz and E. Domany, *Phase transitions in an exactly soluble one-dimensional asymmetric exclusion model*, J. Stat. Phys. **72** (1993) 277–296.

[4] M. Biehl, this volume.

[5] J. Krug, this volume.

[6] P. Politi and J. Villain, *Ehrlich-Schwoebel instability in molecular-beam epitaxy: A minimal model*, Phys. Rev. B **54** (1996) 5114–5129.

[7] G. Ehrlich and F.G. Hudda, *Atomic view of surface diffusion: Tungsten on Tungsten*, J. Chem. Phys. **44** (1966) 1036–1099.

[8] L. Schwoebel and E.J. Shipsey, *Step motion on crystal surfaces*, J. Appl. Phys. **37** (1966) 3682–3686.

[9] M. Siegert, *Ordering dynamics of surfaces in molecular beam epitaxy*, Physica A **239** (1997) 420–427.

[10] W.W. Mullins, *Flattening of a Nearly Plane Solid Surface Due to Capillarity*, J. Appl. Phys. **30** (1959) 77–83.

[11] J. Villain, *Continuum models of crystal growth form atomistic beams with and without desorption*, J. de Physique I **1** (1991) 19–42.

[12] O. Pierre-Louis, M.R. D'Orsogna, and T.L. Einstein, *Edge diffusion during growth: The kink Ehrlich-Schwoebel effect and resulting instabilities*, Phys. Rev. Lett. **82** (1999) 3661–3664.

[13] J. Kallunki, J. Krug, M. Kotrla, *Competing mechanisms for step meandering in unstable growth*, Phys. Rev. B **65** (2002) 205411.

[14] P. Politi and J. Krug, *Crystal symmetry, step-edge diffusion, and unstable growth*, Surface Science **446** (2000) 89–97.

[15] P. Politi and J. Villain, *Kinetic coefficients in a system far from equilibrium*, in *Surface Diffusion: atomistic and collective processes*, Ed. M.C. Tringides, Plenum Press, New York (1997) 177–189.

[16] S. van Dijken, L.C. Jorritsma, and B. Poelsema, *Steering-Enhanced Roughening during Metal Deposition at Grazing Incidence*, Phys. Rev. Lett. **82** (1999) 4038–4041.

[17] J. Yu, J.G. Amar, and A. Bogicevic, *First-principles calculations of steering forces in epitaxial growth*, Phys. Rev. B **69** (2004) 113406.

[18] W.K. Burton, N. Cabrera, F.C. Frank, *The growth of crystals and the equilibrium of their surfaces*, Phil. Trans. Roy. Soc. London A **243** (1951) 299–358.

[19] P. Šmilauer, M. Rost, and J. Krug, *Fast coarsening in unstable epitaxy with desorption*, Phys. Rev. E **59** (1999) R6263–R6266.

[20] M. Rost (2004), unpublished.

[21] D.E. Wolf, *Computer simulation of molecular-beam epitaxy*, in *Scale Invariance, Interfaces and Non-Equilibrium Dynamics*, Eds. A.J. McKane, M. Droz, J. Vannimenus, and D.E. Wolf, Plenum Press, New York (1995).

[22] E. Somfai, D.E. Wolf, and J. Kertész, *Correlated island nucleation in layer-by-layer growth*, J. de Physique I **6** (1996) 393–401.

[23] M. Siegert, *Coarsening dynamics of crystalline thin films*, Phys. Rev. Lett. **81** (1998) 5481–5484.

[24] D. Moldovan and L. Golubovic, *Interfacial coarsening dynamics in epitaxial growth with slope selection*, Phys. Rev. E **61** (2000) 6190–6214.

[25] P. Politi, G. Grenet, A. Marty, A. Ponchet, and J. Villain, *Instabilities in crystal growth by atomic or molecular beams*, Physics Reports **324** (2000) 271–404.

[26] M. Rost and J. Krug, *Coarsening of surface structures in unstable epitaxial growth*, Phys. Rev. E **55** (1997) 3952–3957.

[27] P. Politi, *Kink dynamics in a one-dimensional growing surface*, Phys. Rev. E **58** (1998) 281–294

[28] L.H. Tang, P. Šmilauer, and D.D. Vvedensky, *Noise-assisted mound coarsening in epitaxial growth*, Eur. J. PhysḂ **2** (1998) 409–412.

[29] H. Kallabis, L. Brendel, J. Krug, J., and D.E. Wolf, *Damping of oscillations in layer-by-layer growth*, Int. J. Mod. Phys. B **31** (1997) 3621–3634.

[30] M. Rost and J. Krug, *Damping of growth oscillations in molecular beam epitaxy: A renormalization group approach*, J. de Physique I **7** (1997) 1627–1638.

Martin Rost
Bereich Theoretische Biologie
Insitut für Zelluläre und Molekulare Botanik
Kirschallee 1, Universität Bonn
D-53115 Bonn, Germany
e-mail: martin.rost@uni-bonn.de